Stem Cell Research 54 (2021) 102429

Contents lists available at ScienceDirect

Stem Cell Research

journal homepage: www.elsevier.com/locate/scr

Generating an iPSC line (with isogenic control) from the PBMCs of an ACTA1 (p.Gly148Asp) nemaline myopathy patient

Peter J. Houweling [a,b], Chantal A. Coles [a,b], Chrystal F. Tiong [a], Bridget Nielsen [a], Alison Graham [a], Penny McDonald [a], Annabelle Suter [a], Adam T. Piers [a], Robin Forbes [a,c,d], Monique M. Ryan [a,b,c,e], Sara E. Howden [a,b], Shireen R. Lamandé [a,b], Kathryn N. North [a,b,*]

[a] *Murdoch Children's Research Institute, Melbourne, Victoria, Australia*
[b] *Department of Pediatrics, The University of Melbourne, Victoria, Australia*
[c] *Royal Children's Hospital, Melbourne, Victoria, Australia*
[d] *Victorian Clinical Genetics Services, The Royal Children's Hospital, Melbourne, Victoria, Australia*
[e] *Medicine, Dentistry and Health Science, The University of Melbourne, Melbourne, Victoria, Australia*

A B S T R A C T

To produce an *in vitro* model of nemaline myopathy, we reprogrammed the peripheral blood mononuclear cells (PBMCs) of a patient with a heterozygous p. Gly148Asp mutation in exon 3 of the *ACTA1* gene to iPSCs. Using CRISPR/Cas9 gene editing we corrected the mutation to generate an isogenic control line. Both the mutant and control show a normal karyotype, express pluripotency markers and could differentiae into the three cell states that represent embryonic germ layers (endoderm, mesoderm and neuroectoderm) and the dermomyotome (precursor of skeletal muscle). When differentiated these cell lines will be used to explore disease mechanisms and evaluate novel therapeutics.

Resource Table

Unique stem cell line identifier	MCRIi024-A and MCRIi024-A-1
Alternative name(s) of stem cell line	Patient iPSC line - ACTA1.1u (MCRIi024-A) Isogenic Control iPSC line - ACTA1.Bbc (MCRIi024-A-1)
Institution	Murdoch Children's Research Institute (MCRI)
Contact information of distributor	Kathryn.north@mcri.edu.au
Type of cell line	iPSC
Origin	Human
Additional origin info required for human ESC or iPSC	*Age: 5* *Sex: male* *Ethnicity:* Australian
Cell Source	PBMC
Clonality	Clonal
Associated disease	Nemaline myopathy
Gene/locus	*ACTA1* p.Gly148Asp
Date archived/stock date	November 2020
Cell line repository/bank	Samples and coded data were supplied by the Melbourne Children's Heart Tissue Bank at the Murdoch Children's Research Institute and The Royal Children's Hospital.
Ethical approval	Royal Children's Hospital HREC Reference Number: HREC/45380/RCHM-2018-154931 RCH HREC Reference Number: 38192

1. Resource utility

The heterozygous ACTA1 p.Gly148Asp human iPSC line, together with its isogenic control, provides an experimental model to explore nemaline myopathy in human cardiac and skeletal muscle tissues *in vitro.*

2. Resource details

Nemaline myopathy (NM) is a heterogeneous group of inherited myopathies caused by mutations in at least 12 different genes. The clinical phenotype of NM rages from a severe congenital onset form, which is typically lethal in early life, through to less severe childhood and adult variants. The most common clinical features include muscle weakness and hypotonia (reduced muscle tone) predominantly affecting the face, neck and proximal (shoulder, pelvis, and upper arms/legs) muscles. Most affected individuals have a myopathic facies, high-arched palate, dysarthria and feeding difficulties. Weakness of the respiratory muscles in NM can be life-threatening (OMIM # 102610). Currently

* Corresponding author.
E-mail address: Kathryn.north@mcri.edu.au (K.N. North).

https://doi.org/10.1016/j.scr.2021.102429
Received 21 May 2021; Received in revised form 11 June 2021; Accepted 13 June 2021
Available online 17 June 2021

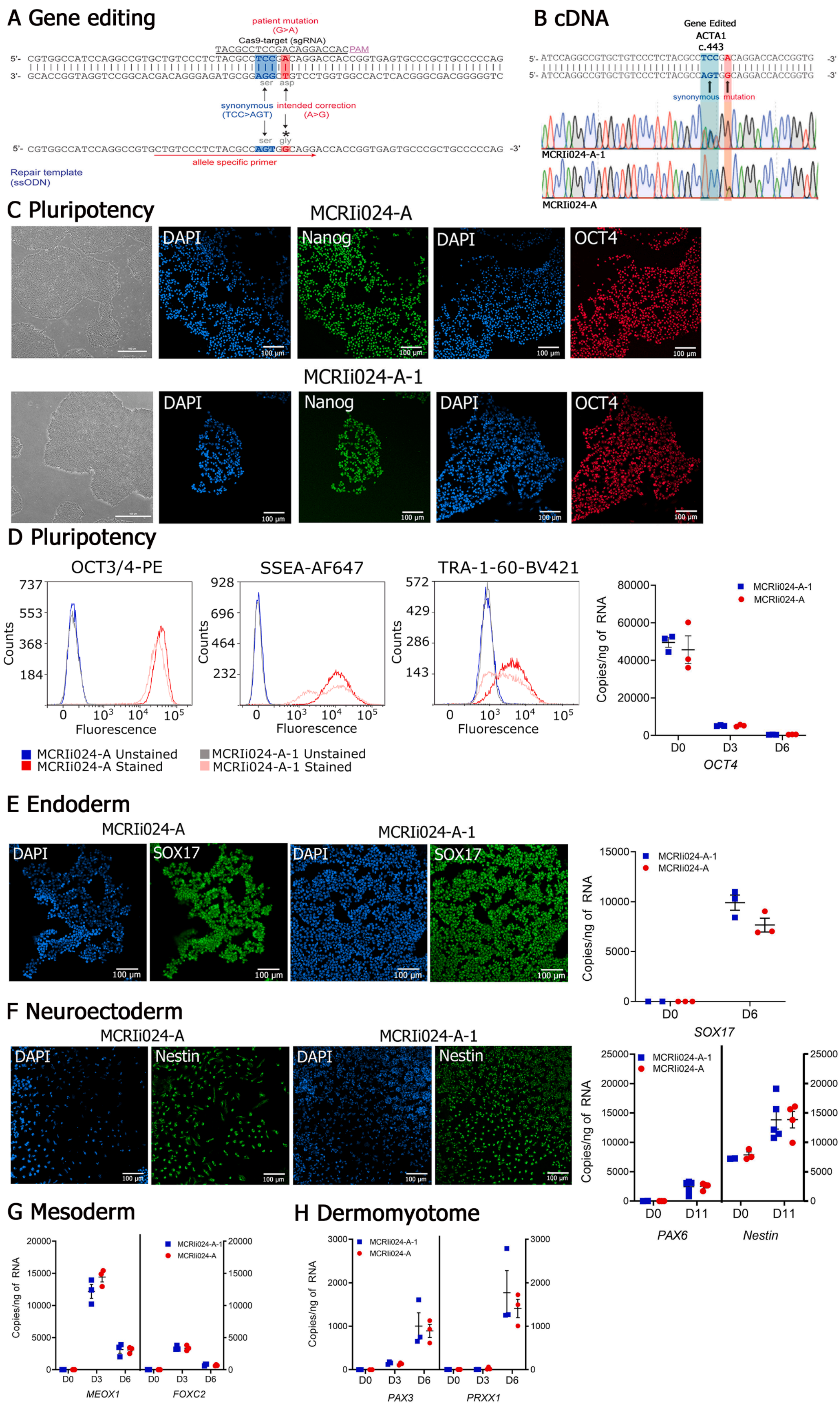

Fig. 1. Molecular and cellular characterization of ACTA1 iPSC lines.

Table 1
Characterization and validation.

Classification	Test	Result	Data
Morphology	Photography Bright field	Normal	Fig. 1 panel C
Phenotype	Qualitative analysis	OCT4 and NANOG positive staining	Fig. 1 panel C
	Quantitative analysis	ACTA1.1u OCT3/4: 99.36% SSEA: 99.54% TRA-1–60: 67.22% ACTA1.Bbc OCT3/4: 98.99% SSEA: 99.35% TRA-1–60: 53.43%	Fig. 1 panel D
Genotype	Karyotype (G-banding) and resolution	Arr(1–22)x22,(X,Y)x1	Supplementary Fig. 1 and Supplementary Fig. 2
Identity	SNPDuo comparative analysis of SNParrays	Identical SNP genotypes (>99.9%) for the entire genome indicating the two samples are from the same individual	Supplementary Fig. 2 and Supplementary Fig. 3
Mutation analysis (IF APPLICABLE)	Sequencing	Heterozygous ACTA1 c.443G>A (p.Gly148Asp) mutation in exon 3 of the ACTA1 gene confirmed in ACTA1.1u	Fig. 1, panel B
Microbiology and virology	Mycoplasma	Both lines confirmed negative by PCR	Supplementary Fig. 1
Differentiation potential	Directed differentiation	Endoderm: SOX17 Ectoderm: Nestin and PAX6 Mesoderm: MEOX1 and FOXC2 Dermomyotome: PRXX1 and PAX3	Fig. 1, panels E-H
List of recommended germ layer markers	Expression of these markers has to be demonstrated at mRNA (RT PCR) or protein (IF) levels, at least 2 markers need to be shown per germ layer	Droplet digital PCR (ddPCR) for mRNA markers and IF have been included for each germ layer and include - OCT4, SOX17, PAX6, Nestin, MEOX1, FOXC2, PAX3 and PRXX1	Fig. 1, panels D-H
Donor screening (OPTIONAL)	HIV 1 + 2 Hepatitis B, Hepatitis C	Not available	Not available
Genotype additional info (OPTIONAL)	Blood group genotyping	Not available	Not available
	HLA tissue typing	Not available	Not available

there is no cure for NM.

The two most common genetic causes of NM are mutations in the genes encoding skeletal α-actin (*ACTA1*) and nebulin (*NEB*). Mutations in skeletal α-actin are responsible for ~26% of all diagnosed cases of NM and the primary cause of the more severe congenital onset myopathies (Sewry et al., 2019).

To improve our understanding of NM disease pathology we generated an iPSC line, with matched isogenic control, from the PBMCs of a patient with a heterozygous c. 443G>A (p.Gly148Asp) mutation in *ACTA1*.

An isogenic control iPSC line, MCRIi024-A-1, was derived from the ACTA1 patient's PBMCs (https://hpscreg.eu/user/cellline/edit/MCRIi024-A) using a one-step reprogramming and gene editing strategy (Wen et al., 2018). Patient PBMCs were co-transfected with episomal reprogramming vectors optimised for derivation of iPSCs from blood, in addition to a plasmid encoding a *ACTA1* pGly148Asp-specific sgRNA, mRNA encoding the Cas9-Gem variant and a 122 bp single-stranded oligodeoxynucleotide (ssODN) repair template comprising ~40 and 80 bp homology arms flanking the mutation (Fig. 1A). Individual iPSC colonies were isolated, expanded and screened by PCR using an allele specific primer that overlaps a 3 bp synonymous change incorporated in the ssODN. The heterozygous *ACTA1* c. 443G>A mutation in transcribed mRNA clone MCRIi024-A was confirmed by Sanger sequencing, along with the correction in MCRIi024-A-1 (Fig. 1B). Both lines also display a normal stem cell morphology, characterised by compact colonies with well-defined cell boundaries (Fig. 1C). Immunofluorescent staining confirmed the expression of pluripotency markers OCT4 and NANOG (Fig. 1C) and flow cytometry confirmed that both the patient and control iPSC lines strongly express pluripotency markers OCT3/4, SSEA4 and TRA-1-60 (Fig. 1D).

Pluripotency of iPSC lines was shown by direct differentiation into the three main germ layers. Definitive endoderm was confirmed by the expression of SOX17 by both immunofluorescence and mRNA transcript expression (Fig. 1E). Neuroectoderm differentiation demonstrated by the presence of NESTIN via immunofluorescence and mRNA expression of both *PAX6* and *Nestin* (Fig. 1F). Finally, differentiation towards a mesoderm lineage is shown by increases in *MEXO1* and *FOXC2* mRNA at day 3 (Fig. 2G) and dermomyotome, by increases in *PAX3* and *PRXX1* mRNA expression at day 6 (Fig. 1H), respectively.

Genome SNP array analysis of both the patient and control line confirmed a stable karyotype (Supplementary Fig. 1) and a SNP Duo analysis also confirmed that MCRIi024-A-1 had >99.9% identity to the parental line MCRIi024-A, indicating that the two lines are from the same individual (Table 1, Supplementary Fig. 1). Both lines were confirmed to be free from mycoplasma contamination (Table 1, Supplementary Fig. 1).

3. Materials and methods

3.1. Cell culture

MCRIi024-A and MCRIi024-A-1 cells were cultured at 37 °C with 5% CO_2 on Matrigel (Corning)-coated plates in Essential 8 (E8) medium (Thermo Fisher Scientific). Media was changed daily, and cells were passaged (1:4 – 1:6) every 3–4 days with 0.5 mM EDTA in PBS.

3.2. CRISPR/Cas9-mediated gene editing of patient PBMCs

Reprogramming and gene-editing factors were introduced into ACTA1 patient PBMCs (MCRI Biobank ID; MCHTB205) using the Neon transfection system (1150 V, 30 ms, 2 pulses). Transfected cells were plated over 3 wells of a matrigel/MEF coated 6-well dish in StemSpan medium. E8 medium, (2 ml) was added to each well 48 hrs post-transfection and half media changes were performed every other day until the cells began to adhere to the plate, when complete media changes were performed.

3.3. PCR screening and sequencing

Gene-corrected clones were identified by allele-specific PCR using primers specific to the gene-corrected *ACTA1* allele. Individual iPSC colonies were picked and expanded in E8 medium. gDNA was extracted from individual iPSC colonies using a DNAeasy Blood and Tissue Kit (Qiagen) according to the manufacturer's instructions. PCR was performed using GoTaq Green Mastermix (Promega) with primer sets specified in Table 2 and an Applied Biosystems (Veriti) 96-well thermocycler. PCR conditions were 95 °C for 3 min, followed by 35 cycles of 95 °C for 18 s, 55 °C for 18 s, 72 °C for 40 s, and then 72 °C for 5 min. PCR products were analysed by agarose gel electrophoresis. PCR products using primers that flank the ACTA1 c. 443G>A mutation site were

Table 2
Reagents details.

	Antibodies used for immunocytochemistry/flow-cytometry		
	Antibody	Dilution	Company Cat # RRID
Pluripotency marker	Rabbit anti-OCT4A (C30A3) monoclonal antibody	1:400	Cell Signaling Technology Catalogue # 2840S RRID AB_2167691
Pluripotency marker	Mouse anti-homeobox Transcription Factor Nanog	1:200	Biolegend Cat# 674202, RRID: AB_2564574
Endoderm marker	Goat anti-Human SOX17 polyclonal antibody	1:100	R&D Systems Cat# AF1924, RRID: AB_2251134
Neuroectoderm marker	Mouse anti-nestin antibody, clone 10C2	1:200	Merck Cat# MAB5326, RRID: AB_2251134
Secondary Antibody	Donkey anti-rabbit IgG (H & L) Alexa Fluor 594	1:1000	Thermo Fisher Scientific Cat# A21207, RRID: AB_141637
Secondary Antibody	Goat anti-mouse IgG (H & L) Alexa Fluor 488	1:1000	Thermo Fisher Scientific Cat# A11029, RRID: AB_2534088
Secondary Antibody	Donkey anti-Goat IgG (H & L) Alexa Fluor 488	1:1000	Thermo Fisher Scientific Cat# A32814, RRID: AB_2762838
FACS antibody	PE Mouse anti-Oct3/4	1:5	BD Biosciences Cat# 560186, RRID: AB_1645331
FACS antibody	Alexa Fluor 647 anti-human SSEA-4 antibody	1:100	BioLegend Cat# 330408, RRID: AB_1089200
FACS antibody	BV421 Mouse Anti-Human TRA-1–60 Antigen	1:20	Becton Dickinson Cat# 562711, RRID: AB_2737738
	Primers	Size of band	Forward/Reverse primer (5′-3′)
	Target		
Pluripotency marker	*OCT4*	261 bp	GAAGTGGGTGGAGGAAGCTG/TAGTCGCTGCTTGATCGCTT
Endoderm marker	*SOX17*	103 bp	GCATGACTCCGGTGTGAATCT/TCACACGTCAGGATAGTTGCAG
Neuroectoderm marker	*PAX6*	163 bp	TTGCTTGGGAAATCCGAG/TGCCCGTTCAACATCCTT
Neuroectoderm marker	*NESTIN*	176 bp	CTGGAGCAGGAGAAACAGGG/CTGAGGGAAGTCTTGGAGCC
Mesoderm marker	*MEOX1*	170 bp	ACTCGGCTCCGCAGATATGA/GAACTTGGAGAGGCTGTGGA
Mesoderm marker	*FOXC2*	248 bp	TGGTATCTCAACCACAGCGG/CCCGGGACACGTCAGTATTT
Dermomyotome marker	*PRXX1*	103 bp	AGGCTTTGGAGCGTGTCTTT/GTTACCTGCACTCTCGCCTC
Dermomyotome marker	*PAX3*	240 bp	CGCTTCCTCCAAGCACTGTA / AGAGCGCGTAATCAGTCTGG
Targeted mutation sequencing	*ACTA1*	450 bp	GTCATGGTCGGTATGGGTCAG/ GCCACGTAGCACAGCTTCTC
Knock-in template (ODN) sequence:		122 bp	CCCAGATCATGTTTGAGACCTTCAACGTGCCCGCCATGTACGTGGCCATCCAGGCCGTGCTGTCCCTCTACGCC**TCCGG**CAGGACCACCGGTGAGTGCCCGCTGCCCCCAGTCCCCTCTCCC

generated (Table 2). Amplicons generated using primers flanking the intended correction (Table 2) and the antisense strand were Sanger-sequenced to confirm correction of the mutation, clonality and/or absence of off target mutations (Fig. 1A).

3.4. RNA extraction and digital droplet quantitative real-time PCR (ddPCR) quantitation

RNA was extracted using RNeasy mini kit (Qiagen). Total RNA was quantitated using TapeStation (Agilent Technologies 2200). Diluted RNA concentrations were then assessed using Qubit 3.0 fluorometer (Thermo Fisher Scientific). All RNA samples were diluted to 25 ng/µl and 1 ng/µl RNA, and 4 µl of 25 ng/µl RNA or 2 µl of 1 ng/µl RNA samples were reverse transcribed to synthesise cDNA using the High-Capacity cDNA Reverse Transcription Kit (Thermo Fisher Scientific) as per manufacturer guidelines.

ddPCR assays were conducted using 2X QX200 ddPCR EvaGreen Supermix (Biorad) in a twin.tec 96-well plate (Biorad) to a final volume of 24 µl for lipid droplet generation. The sample plate of droplets was placed in a thermal cycler (T100, BioRad) for subsequent PCR amplification using gene-specific primers outlined in Table 2. The thermal cycling conditions were as follows: 1 activation cycle of 5 min at 95 °C, 40 denaturation cycles of 30 sec at 96 °C and annealing cycles of 1 min at 55–60 °C depending on the target gene of interest, a post-cycling step of signal stabilisation of 5 min at 4 °C followed by 5 min at 90 °C. All cycling steps were performed using a 2 °C per sec ramp rate. Following PCR amplification, the sample plate was loaded on the QX200 Droplet reader (Biorad) and the assay information was entered into the QuantaSoft (BioRad) software.

3.5. Immunocytochemistry

Cells were fixed in 4% paraformaldehyde for 20 min at room temperature then permeabilized with 0.1% Triton X-100 in PBS for 10 min at room temperature. Non-specific binding was blocked with 3% bovine serum albumin in PBS overnight at 4 °C. Cells were incubated with primary antibodies for 2 h at room temperature, followed by secondary antibodies for 60 min (Table 2). Nuclei were stained with DAPI (1 µg/ml) and cells visualised with a fluorescent microscope.

3.6. Flow cytometry

Cells were dissociated with TrypLE (Thermo Fisher Scientific) and incubated with conjugated antibodies to cell surface proteins TRA-1–60 and SSEA4 (Table 2) diluted in PBS containing 2% foetal bovine serum (FBS) for 15 min at 4 °C. Cells were washed with 2% FBS in PBS, then fixed and permeabilized using the eBioscienceTM Foxp3/Transcription Factor Staining buffer set (Thermo Fischer Scientific), then stained with a conjugated antibody to intracellular OCT3/4 (Table 2). Samples were analysed using a LSR Fortessa X20 (BD Biosciences) and BD FACSDiva and FCS Express software.

3.7. Directed differentiation (endoderm, neuroectoderm, mesoderm and dermomyotome)

iPSCs were differentiated in monolayer culture into either endoderm for 6 days (Loh et al., 2014), anterior neuroectoderm for 12 days (Tchieu et al., 2017), or mesoderm for 3 days and dermomyotome for 6 days (Matsuda et al., 2020). Differentiation was assessed by immunocytochemistry and/or mRNA expression using ddPCR for lineage-specific markers.

3.8. Molecular karyotyping, SNP analysis and Mycoplasma detection

Cell pellets were provided to the Victorian Clinical Genetics Service (Murdoch Children's Research Institute, Melbourne, Australia) and genomic DNA was analysed using an Infinium GSA-24 v1.0 SNP array (Illumina). Mycoplasma contamination was assessed by PCR (Cerberus Sciences, Adelaide, Australia).

Declaration of Competing Interest

The authors declare the following financial interests/personal relationships which may be considered as potential competing interests: Peter Houweling reports financial support was provided by Murdoch Childrens Research Institute. Peter Houweling reports a relationship with Murdoch Childrens Research Institute that includes: employment.

Data availability

Data will be made available on request.

Appendix A. Supplementary data

Supplementary data to this article can be found online at https://doi.org/10.1016/j.scr.2021.102429.

References

Loh, K.M., Ang, L.T., Zhang, J., Kumar, V., Ang, J., Auyeong, J.Q., Lee, K.L., Choo, S.H., Lim, C.Y., Nichane, M., Tan, J., Noghabi, M.S., Azzola, L., Ng, E.S., Durruthy-Durruthy, J., Sebastiano, V., Poellinger, L., Elefanty, A.G., Stanley, E.G., Chen, Q., Prabhakar, S., Weissman, I.L., Lim, B., 2014. Efficient endoderm induction from human pluripotent stem cells by logically directing signals controlling lineage bifurcations. Cell Stem Cell 14 (2), 237–252.

Matsuda, M., Yamanaka, Y., Uemura, M., Osawa, M., Saito, M.K., Nagahashi, A., Nishio, M., Guo, L., Ikegawa, S., Sakurai, S., Kihara, S., Maurissen, T.L., Nakamura, M., Matsumoto, T., Yoshitomi, H., Ikeya, M., Kawakami, N., Yamamoto, T., Woltjen, K., Ebisuya, M., Toguchida, J., Alev, C., 2020. Recapitulating the human segmentation clock with pluripotent stem cells. Nature 580 (7801), 124–129.

Sewry, C.A., Laitila, J.M., Wallgren-Pettersson, C., 2019. Nemaline myopathies: a current view. J. Muscle Res. Cell Motility 40 (2), 111–126.

Tchieu, J., Zimmer, B., Fattahi, F., Amin, S., Zeltner, N., Chen, S., Studer, L., 2017. A modular platform for differentiation of human PSCs into all major ectodermal lineages. Cell Stem Cell 21 (3), 399–410.e397.

Wen, W., Cheng, X., Fu, Y., Meng, F., Zhang, J.P., Zhang, L., Li, X.L., Yang, Z., Xu, J., Zhang, F., Botimer, G.D., Yuan, W., Sun, C., Cheng, T., Zhang, X.B., 2018. High-level precise knockin of iPSCs by simultaneous reprogramming and genome editing of human peripheral blood mononuclear cells. Stem Cell Reports 10 (6), 1821–1834.